Isotopic Selectivity in Ultrathin Langmuir–Blodgett Membranes of a Cross-Linked Cellulose Derivative

A. R. Esker,*,†,∥ H. Grüll,*,†,⊥ G. Wegner,§ S. K. Satija,‡ and C. C. Han†

Polymers Division and NIST Center for Neutron Research, National Institute of Standards and Technology, Gaithersburg, Maryland 20899, Max-Planck Institut für Polymerforschung, Ackermann Weg 10, D-55128 Mainz, Germany, and Virginia Polytechnic Institute and State University, Department of Chemistry, Blacksburg, Virginia 24061-0212

Cross-linked Langmuir–Blodgett films of isopentylcellulose cinnamate (IPCC) sandwiched between a polymeric diffusion couple provide an ideal system for probing fundamental transport processes across ultrathin (≈6 nm) membranes. Neutron reflectivity experiments for polystyrene/IPCC/polystyrene trilayers (with one perdeuterated polystyrene layer) reveal that the isotopically labeled (perdeuterated) species crosses the membrane faster than normal polystyrene of the same size resulting in displacement of the free-standing membrane. Mismatched polystyrene molecular masses confirm isotopic selectivity and also indicate size discrimination by the membrane. The membrane displacement is reminiscent of but different from Kirkendall effect experiments in metallic systems and marker displacement studies in polymers.

Introduction

Studies of molecular transport across membranes and interfaces provide an area of intense theoretical, experimental, and technological interest. One of the landmark experimental studies in this area was the observation of the Kirkendall effect in metallic systems.[1] The Kirkendall experiment showed that copper (A) and zinc (C) in a brass diffusion couple had different diffusion coefficients through the displacement of an oxide impurity (B) located at the interface. This work fostered additional studies of the type A/B/C, where the "/" represents a distinct interface in trilayer geometries, to examine isotopic effects and void facilitated diffusion in metallic systems.[2,3] More recently, films of type A/B/C, where A and C are polymers and B is a vapor-deposited layer of gold particles, have been of interest.[4–9] In early studies,[4,5] displacement of the gold particles from their initial interfacial position during depth profiling experiments was taken as a sign that polymer interdiffusion could be attributed[4,5] to a compressible rather than incompressible[10] mechanism by including void transport across the interface. Subsequent experiments utilizing isotopic labeling on A/B films without markers were used to test various predictions for polymer dynamics following from the theory of reptation.[11–15] One basic assumption for eliminating the incompressible mechanism was that the gold particles are inert. Recent studies[8,9] of gold particle marker displacement show substantial retardation of gold particle mobility and to a lesser extent polymer mobility resulting from bridge formation between metal and polymer.

In contrast to the experiments above where the markers might be inert, systems of type A/B/C where B is a membrane or network clearly are not. Transport processes across synthetic membranes are relevant for separating liquids, gases, electrolytes, and even isotopes arising from subtle differences in the interactions between diffusants and the membrane.[16–20] The transport of small and large molecules across natural membranes in biological and biomimetic systems is important in cellular processes[21–23] and for sensor applications.[24,25] An important feature of the biological systems is the fact that the membrane is only ≈5 nm thick. Other examples where the transport of polymeric species across and into barrier layers plays an important role is organic-based microelectronics such as field effect transistors of type A/B/A and photoluminescence devices prepared through layer by layer deposition processes.[26,27] In the microelectronics systems, a

* To whom correspondence should be addressed. E-mail: aesker@vt.edu; holger.gruell@philips.com.
† Polymers Division, National Institute of Standards and Technology.
‡ NIST Center for Neutron Research, National Institute of Standards and Technology.
§ Max-Planck Institut für Polymerforschung.
∥ Virginia Polytechnic Institute and State University.
⊥ Permanent address: Philips Research Laboratories, 5656 AA Eindhoven, The Netherlands.

(1) Smigelskas, A. D.; Kirkendall, E. O. *Trans. Am. Inst. Min. Eng.* **1947**, *171*, 130.
(2) Tuijn, C. *Defect Diffus. Forum*, **1997**, *141*, 1.
(3) Morral, J. E.; Son, Y.-H.; Thompson, M. S. *Acta Metall.* **1988**, *36*, 1971.
(4) Kramer, E. J.; Green, P. F.; Palmstrøm, C. J. *Polymer* **1988**, *25*, 473.
(5) Green, P. F.; Palmstrøm, C. J.; Mayer, J. W.; Kramer, E. J. *Macromolecules* **1985**, *18*, 501.
(6) Reiter, G.; Huttenbach, S.; Foster, M.; Stamm, M. *Macromolecules* **1991**, *24*, 1179.
(7) Liu, Y.; Reiter, G.; Kunz, K.; Stamm, M. *Macromolecules* **1993**, *26*, 2134.
(8) Cole, D. H.; Shull, K. R.; Rehn, L. E.; Baldo, P. *Phys. Rev. Lett.* **1997**, *26*, 5006.
(9) Cole, D. H.; Shull, K. R.; Baldo, P.; Rehn, L. *Macromolecules* **1999**, *32*, 771.

(10) Brochard, F.; Jouffroy, J.; Levinson, P. *Macromolecules* **1983**, *16*, 1638.
(11) de Gennes, P. G. *J. Chem. Phys.* **1971**, *55*, 572.
(12) Composto, R. J.; Kramer, E. J.; White, D. M. *Nature* **1987**, *328*, 234.
(13) Russell, T. P. et al. *Nature* **1993**, *365*, 235.
(14) Klein, J. *Science* **1990**, *250*, 640.
(15) Reiter, G.; Steiner, U. *J. Phys. II* **1991**, *1*, 659.
(16) Tieke, B. *Adv. Mater.* **1991**, *3*, 532.
(17) Koros, W. J.; Coleman, M. R.; Walker, D. R. B. *Annu. Rev. Mater. Sci.* **1992**, *22*, 47.
(18) Hendel, R. A.; Nomura, E.; Janout, V.; Regen, S. L. *J. Am. Chem. Soc.* **1997**, *119*, 6909.
(19) Chmielewski, A. G.; Zakrzewskatrznadel, G.; Miljevic, N. R.; Vanhook, W. A. *J. Membr. Sci.* **1991**, *60*, 319.
(20) Krasemann, L.; Tieke, B. *Langmuir* **2000**, *16*, 287.
(21) Green, D. R.; Reed, J. C. *Science* **1998**, *281*, 1309.
(22) Lubensky, D. K.; Nelson, D. R. *Biophys. J.* **1999**, *77*, 1824.
(23) DeCoursey, T. E.; Cherny, V. V. *J. Gen. Physiol.* **1997**, *109*, 415.
(24) Cornell, B. A. et al. *Nature* **1997**, *387*, 580.
(25) Sackmann, E. *Science* **1996**, *271*, 43.
(26) Yang, Y.; Heeger, A. J. *Nature* **1994**, *372*, 344.

Table 1. Weight-Average Molecular Masses of the Polystyrene Samples Used in This Study

	stated[a]			measured by GPC[b,f]		
code	M_w[c] (kg mol^{-1})	M_w/M_n[d]	n_w[e]	M_w[c] (kg mol^{-1})	M_w/M_n[d]	n_w[e]
40 k dPS	40.0	1.02	357	40.2	≤1.03	359
39 k hPS	39.0	1.02	375	37.5	≤1.03	361
28 k hPS	28.5	1.03	274	28.1	≤1.03	270

[a] Polymer Laboratories, Inc. [b] Measured by Dr. Qing Gi at the Virginia Polytechnic Institute and State University by gel permeation chromatography (GPC) against regular polystyrene standards in *N*-methyl pyrrolidone on a Waters 150C instrument with a differential viscometric detector. [c] M_w = weight-average molecular mass [10]. [d] M_w/M_n = polydispersity index. [e] n_w = weight-average degree of polymerization. [f] The relative error in the measured data is about 4%.

certain degree of interpenetration arising from processing conditions and interdiffusion between conducting and insulating layers is necessary to ensure charge transport across the entire device.

This letter details our efforts to develop membranes of biological dimension (≈6 nm) to study polymer dynamics in ultrathin films of the type A/B/C. As we will demonstrate below, the membranes behave like markers[1−9] in terms of analytical sensitivity for novel neutron reflectivity experiments but also exhibit isotopic selectivity.[16,19,23] By use of polymeric diffusants, defect problems, like those encountered using gases to probe membranes this thin, were avoided.[18] The results discussed below are not only relevant to the systems noted above but also will serve as important tools for probing predictions of how membrane thicknesses on the order of a diffusing polymer's radius of gyration alter the mechanism of polymer transport.[28,29]

Experimental Section

A detailed experimental description is available free of charge from the Internet (http://pubs.acs.org) as Supporting Information. To prepare these samples, polymer A, a polystyrene sample (≈50 nm thick), is spin-coated from a toluene solution onto a hydrophobic silicon (Si) wafer and is annealed for 2 h at 120 °C to ensure removal of the solvent. Specific polystyrene properties (Polymer Laboratories, Inc.)[30] are summarized in Table 1.[31] Next, a 6 nm thick membrane M of isopentylcellulose cinnamate[32] is transferred by LB onto A. The membrane is subsequently photocross-linked to form a network.[33] Polymer B, a second polystyrene sample of a thickness 80 < d/nm < 100, is then floated on top of M to form a trilayer air//B/M/A//Si as schematically shown in Figure 1A. The trilayer configuration A/M/B facilitates investigations of how an ultrathin interstitial layer M affects the interdiffusion of A and B under well-defined conditions.

Results and Discussion

For the first experiment, the diffusants were kept as chemically and physically similar as possible by employing

isotopic labeling with 39 k polystyrene (hPS) and 40 k perdeuterated polystyrene (dPS), where k is short for kg mol^{-1}, serving as polymers B and A, respectively. This polymer pair was separated by six LB layers of isopentylcellulose cinnamate (IPCC) to construct the system

$$\text{air}//\text{hPS (39 k)}/\text{IPCC (5.7 nm)}/\text{dPS (40 k)}//\text{Si} \quad (A)$$

This layered configuration is well suited for depth profiling using neutron reflectivity, NR.[34] Figure 2 shows experimental reflectivity curves, $R(q)$, as a function of the scattering wave vector, $q = (4\pi/\lambda) \sin\theta$, where λ is the wavelength and θ is both the incident and reflected angle, for configuration A. The corresponding scattering length density (SLD) profiles, (b/V) versus d, where d is the distance into the sandwich measured from the air interface, were used to generate the calculated fits of the reflectivity profiles (solid lines on the $R(q)$ versus q plots in Figure 2).[35] SLD is used here instead of volume fraction, ϕ (composition), as the relationship for the binary regions $(b/v)_{average} = \phi_{dPS}(b/v)_{dPS} + \phi_{hPS}(b/v)_{hPS}$ where $\phi_{dPS} + \phi_{hPS} = 1$ is uniquely definable but the ternary membrane region $(b/v)_{average} = \phi_{dPS}(b/v)_{dPS} + \phi_{hPS}(b/v)_{hPS} + \phi_{IPCC}(b/v)_{IPCC}$ where $\phi_{dPS} + \phi_{hPS} + \phi_{IPCC} = 1$ is not. As the SLD contrasts between the dPS/Si and IPCC/dPS interfaces are much larger than that at the hPS/IPCC and air/hPS interfaces, the spacing of the Keissig fringe maxima is dominated by interference between the IPCC/dPS and dPS/Si interfaces at early times. Hence, the periodicity of the fringes corresponds to the thickness of the dPS film at early times. The reflectivity and the corresponding SLD profile used to fit the NR data for the initial sample before any annealing are shown in Figure 2A. The small dip in the center of the SLD profile indicates the position of the membrane as IPCC has the lowest SLD in the trilayer. Figure 2B shows a representative snapshot after annealing 10 min at 20 °C above the glass transition temperature for PS ($T_g \approx 100$ °C) and rapidly quenching the system to room temperature ($T < T_g$) for NR measurements. As can be seen in Figure 2B relative to Figure 2A, the spacing of the Kiessig fringes increases. Independent of fitting, this indicates that the dPS layer shrinks. The fitting analysis reveals that the magnitude of the displacement of the membrane center toward the Si substrate is about 4 nm. The membrane itself has swollen to almost twice its initial thickness. Upon further annealing, more bumps appear in the reflectivity profile (Figure 2C) as the polymers eventually interdiffuse and mix whereby the interference of neutrons reflected from all interfaces contribute to the measured intensity. The corresponding SLD profile shows that the membrane position is ultimately displaced toward the Si by a total of 16 nm. Additionally, there is an indication of dPS enrichment at the air interface, and a dPS-rich layer remains in the vicinity of the Si wafer surface. The segregation of dPS to the air interface is consistent with previous studies of dPS/hPS mixtures in thin films,[36] while a dPS layer at the Si surface may be a kinetic effect.[37] After reaching equivalent polymer concentrations on both sides of the membrane, the membrane displacement ceases. This final state is schematically shown in Figure 1B. The membrane displacement indicates a greater flux of dPS through the membrane than hPS suggesting an isotopic selectivity for polymer transport across the

(27) Baur, J. W.; Rubner, M. F.; Reynolds, J. R.; Kim, S. *Langmuir* **1999**, *15*, 6460.

(28) Yoon, H.; Deutsch, J. M. *J. Chem. Phys.* **1995**, *102*, 9090.

(29) Lee, N.; Obukhov, S. *J. Phys. II France* **1996**, *6*, 195.

(30) Certain commercial materials and instruments are identified in this article to adequately specify the experimental procedure. In no case does such identification imply recommendation or endorsement by the National Institute of Standards and Technology, nor does it imply that materials or equipment identified are necessarily the best available for the purposes.

(31) According to ISO 31-8, the term "molecular weight" (M_w) has been replaced with "relative molecular mass", symbol $M_{r,w}$. The conventional notation rather than ISO notation has been employed for this article.

(32) Schaub, M. Ph.D. Thesis, University of Mainz, Mainz, Germany, 1993.

(33) Iida, S.; Schaub, M.; Schulze, M.; Wegner, G. *Adv. Mater.* **1993**, *5*, 564.

(34) Russell, T. P. *Mater. Sci. Rep.* **1990**, *5*, 171.

(35) Welp, K. A.; Co, C.; Wool, R. P. *J. Neutron Res.* **1999**, *8*, 37.

(36) Hariharan, A.; Kumar, S. K.; Rafailovich, M. H.; Sokolov, J.; Zheng, X.; Duong, D.; Schwarz, S. A.; Russell, T. P. *J. Chem. Phys.* **1993**, *99*, 656.

(37) Lin, E. K.; Kolb, R.; Satija, S. K.; Wu, W. L. *Macromolecules* **1999**, *32*, 3753.
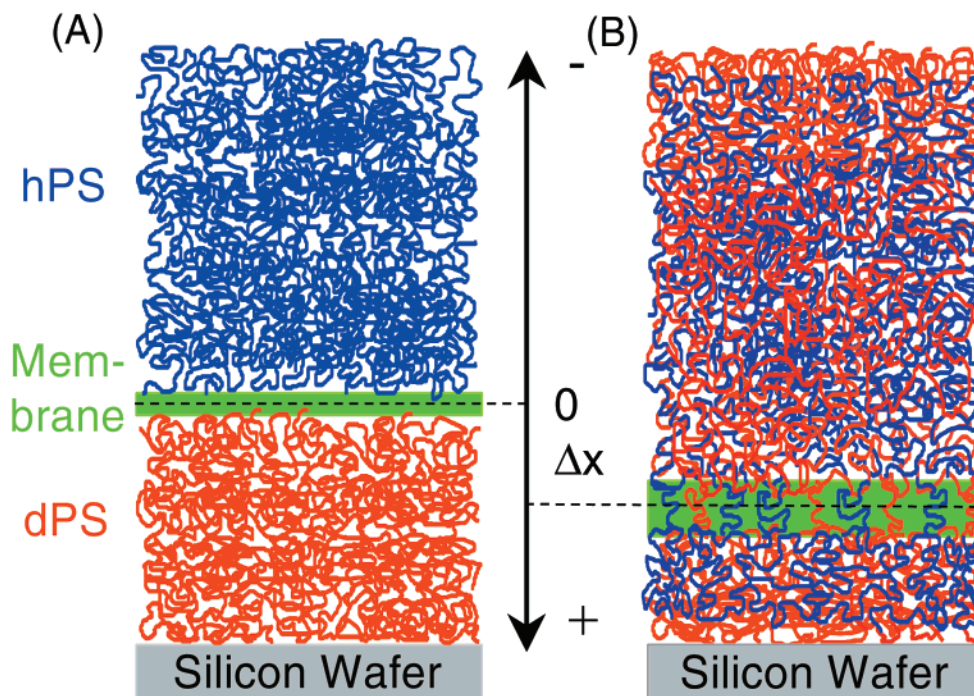
Figure 1. A schematic depiction of membrane displacement during membrane-mediated interdiffusion for config A. The dPS and hPS layers, initially (A) separated by the IPCC membrane, mix upon annealing. Mixing swells the membrane by a factor of ≈2 and ultimately displaces the membrane by a distance of Δx, the distance the membrane moves relative to its initial distance from the silicon wafer (positive values indicate movement toward silicon), as dPS crosses faster than hPS (B). Additionally, a kinetically stable dPS layer is found at the silicon wafer and also at the air interface where dPS adsorbs.
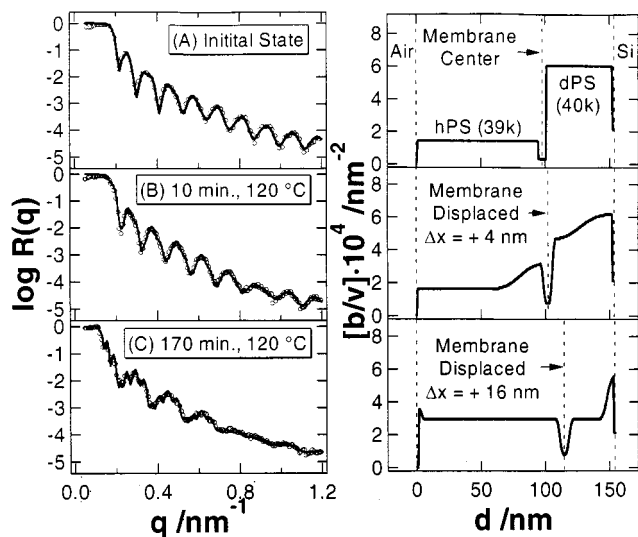

Figure 2. Representative reflectivity and model SLD profiles for config A at three annealing times. The three graphs on the left-hand side of the figure show the reflectivity data (circles) and best fits of the data (solid lines) based on the corresponding model SLD profile given to the right for (a) 0, (b) 10, and (c) 170 min of annealing at 120 °C. At $q < 0.8$ nm^{-1}, the standard deviation in the data is smaller than the symbol size. At the highest q values, the standard deviations correspond to half a decade on a logarithmic scale at most. The graph clearly shows displacement of the membrane (the dip in the SLD) toward the silicon substrate.

membrane. The nearly exponential time dependence of the membrane position is seen in Figure 3. We also tested the reversed configuration

air//dPS (40 k)/IPCC (5.7 nm)/hPS (39 k)//Si   (B)

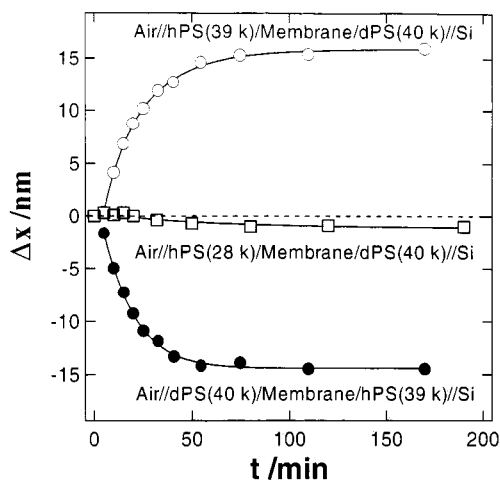where the deuterated polymer is on top of the trilayer.

Figure 3. Membrane displacement kinetics, Δx (as defined in Figure 1) vs t, for configs A, B, and D. The nearly exponential displacement observed in config A (open circles) is reversed in direction but is of comparable magnitude for the inverted configuration, B (filled circles). In contrast, the use of mismatched molecular weights, config D (open squares), results in very little displacement of the membrane. Similarly, blank experiments not shown in the figure (no membrane), configs C and E, exhibit no significant displacement of the interface. The standard deviation of the data points is less than the symbol size.

The experimental data and fitting were similar to those used for Figure 2 with two major exceptions. Instead of the dPS layer at the Si surface, there was now a hPS layer at the surface. More importantly, the membrane displacement is now reversed toward the air (dPS layer) but with the same exponential displacement kinetics and magnitude as shown in Figure 3. Thus, surface effects, such as a shift in T_g in thin films, the "sticky" layer next to the substrate, or effects of the dPS enrichment at the air interface can be excluded and strongly suggest that

the origin for the displacement is isotopic selectivity by the membrane.

While the displacement of the membrane may seem similar to the classical Kirkendall effect[1] and to metallic and polymeric marker experiments,[4-9] the origin of the phenomena observed here is different. In experiments with matched molecular masses of dPS and hPS, the tracer diffusion coefficients of A and B are essentially the same, $D_{A,tracer} = D_{B,tracer}$. Both metallic and polymeric marker systems show no displacement of the interface when the tracer diffusion coefficients of both components are equal, while we observe a large membrane displacement. A control experiment using the same polymers but without the membrane,

$$\text{air//hPS (39 k)/dPS (40 k)//Si} \qquad \text{(C)}$$

which was annealed at a low enough temperature ($T = 103\ °C$), thereby slowing down the interdiffusion enough to observe the early broadening of the interface, shows no significant displacement (± 0.4 nm) of the interface over the range of interfacial broadening accessible by NR. This observation is consistent with other interdiffusion experiments of isotopic mixtures.[13-15] If the mechanism leading to membrane displacement would be similar to those hypothesized for marker displacement experiments, that is, a flux of voids accompanying mass transport, a displacement of the interface should not occur as $D_A = D_B$ which is consistent with the stable interfacial position in the absence of the membrane. The different interactions with the membrane which would be regarded as inert in marker experiments result in different transport properties for A and B through M such that $P_{A\ through\ M} > P_{B\ through\ M}$ (P is the permeation coefficient). Hence, subtle differences in the interactions of the polymers with the membrane resulting from the isotopic labeling provide the driving force for membrane displacement due to faster transport of the deuterated species.

An additional experiment which demonstrates that the different transport rate of A and B through M drives the membrane displacement is the interdiffusion of 28 k hPS and 40 k dPS, through the IPCC membrane,

$$\text{air//hPS (28 k)/IPCC (5.7 nm)/dPS (40 k)//Si} \quad \text{(D)}$$

In this experiment, the tracer diffusion coefficients are clearly inequivalent, $D_{A,tracer} \neq D_{B,tracer}$. If the mechanism were the same as in the Kirkendall or polymeric marker experiments, we would expect a displacement of the interface both with and without the membrane. However, the NR measurements (Figure 4) for three different annealing times at $T = 120\ °C$ show almost no displacement of the membrane (Figure 3), demonstrating that the transport rate of 28 k hPS and 40 k dPS across the membrane is essentially the same, $P_{A\ through\ M} = P_{B\ through\ M}$. Thus, the faster transport of 28 k hPS through the membrane relative to 39 k hPS resulting from decreasing size ($\approx 25-30\%$ difference in self-diffusion coefficients assuming nonentangled dynamics) is almost quantitatively equivalent to the faster transport of 40 k dPS through the membrane relative to 39 k hPS arising from an isotopic effect. A NR interdiffusion experiment using polymers of mismatched molecular masses and no membrane,

$$\text{air//hPS (28 k)/dPS (40 k)//Si} \qquad \text{(E)}$$

shows no significant displacement, within ± 0.4 nm, of the polymer/polymer interface upon annealing at $T = 103\ °C$. In comparison with configuration C, the mutual
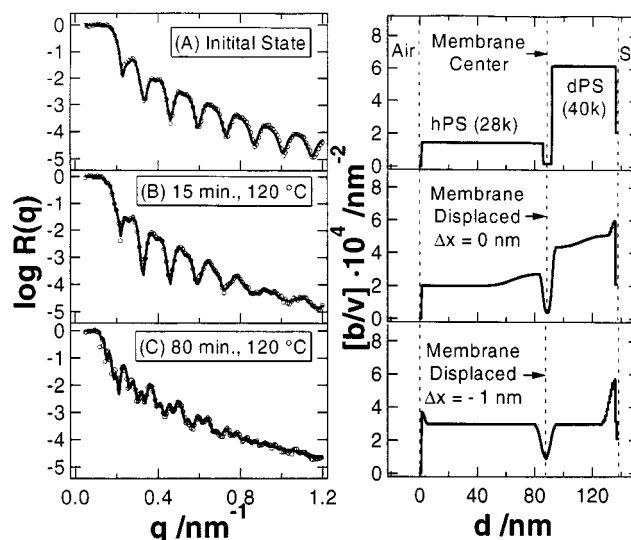

Figure 4. Representative reflectivity and model SLD profiles for config D at three annealing times. The three graphs on the left-hand side of the figure show the reflectivity data (circles) and best fits of the data (solid lines) based on the corresponding model SLD profile given to the right for (a) 0, (b) 10, and (c) 170 min of annealing at 120 °C. In contrast to Figure 2, there is almost no displacement of the interface. Experimental errors are of the same magnitude as those described in the legend of Figure 2.

diffusion coefficient is relatively larger by about 30%, as expected, reflecting the molecular mass mismatch with a smaller sample. This opens a new question regarding the mechanism of marker displacement experiments. Either the explanation used for marker displacement is not entirely correct, that is, markers are not absolutely inert and do have interactions with the polymers (e.g., size discrimination), or the effect is too small for this special polymer pair to be detected by NR.

The most interesting aspect of this work is that isotopic labeling has a large effect on transport across a membrane. While isotopic effects play a key role in phenomena which are sensitive to the nuclear structure or bond polarizability, isotopic labeling provides an important tool in NMR, IR, NR, nuclear reaction analysis, secondary ion mass spectrometry, and so forth. Nonetheless, the use of these tools is often based on the assumption that the chemical and bulk physical properties of the isotopically labeled materials are not significantly altered. In particular, polymer science routinely utilizes deuterium-labeled polymers to probe thermodynamic and structural properties although care has been taken to account for isotopic effects. Examples of this include small-angle neutron scattering experiments suggesting that isotopic blends could undergo phase separation[38] and thin film experiments demonstrating that isotopic differences could lead to preferential adsorption at surfaces and to a layered structure upon phase separation in dPS/hPS pairs as well as other polymer systems.[39-41] These effects have been explained in terms of the collective contribution of small differences in polarizability and molar volume between C–H and C–D bonds to create a slightly positive monomer–monomer interaction parameter, χ_{AB}.[38] For the

(38) Bates, F. S.; Wignall, G. D. *Phys. Rev. Lett.* **1986**, *57*, 1429.

(39) Budkowski, A.; Steiner, U.; Klein, J. *J. Chem. Phys.* **1992**, *97*, 5229.

(40) Budkowski, A.; Steiner, U.; Klein, J.; Schatz, G. *Europhys. Lett.* **1992**, *18*, 705.

(41) Klein, J.; Kerle, T.; Zink, F.; Eiser, E. *Macromolecules* **2000**, *33*, 1298.

membrane system, we are dealing with a ternary phase diagram where the relevant interactions are between IPCC, dPS, and hPS. In terms of interaction parameters, this reduces to $\chi_{IPCChPS}$, $\chi_{IPCCdPS}$, and χ_{hPSdPS}. For the case of polystyrene, χ_{dPShPS} can be estimated to be a very small value, on the order of 2×10^{-4} at 120 °C.[38] Decreasing entropies of mixing with increasing polymer molecular masses are reflected in the expression of the critical value of the interaction parameter $\chi_{AB,c} = 0.5(n_A^{-1/2} + n_B^{-1/2})^2$. For the present case, $\chi_{AB,c} = 0.5(n_A^{-1/2} + n_B^{-1/2})^2 \approx 6 \times 10^{-3}$,[42] where the weight-average degrees of polymerization are $n_A = 359$ and $n_B = 361$ for matched dPS and hPS, respectively, is at least a factor of 10 larger, indicating the system is far above its upper critical solution temperature. Although the effects on the dPS/hPS interaction are negligible, it is reasonable to conclude that $\chi_{IPCChPS} \neq \chi_{IPCCdPS}$, reflecting differences in monomer−monomer interactions. The difference in χ_{AB} upon isotopic labeling then results in a greater dPS flux through the IPCC membrane for the matched molecular weight. This conclusion is consistent with shifts seen in the phase diagrams of blends between other polymer pairs, like polystyrene and poly(vinylmethyl ether) upon the isotopic labeling of PS.[43] Even though χ_{AB} can depend on molecular mass,[44] the predominant effect arises from the chemical groups present in the monomer structure. Hence, it is reasonable to assume that the magnitude of $\chi_{IPCChPS}$ and $\chi_{IPCCdPS}$ will be retained for different molecular masses even down to monomer sizes. Precedence for isotopic effects on transport is also found in studies of small molecule systems.[2,19,23]

Conclusions

In conclusion, large differences in dPS and hPS transport rates across ultrathin membranes were observed in NR experiments suggesting that the transport properties through ultrathin membranes as well as polymer dynamics in confined geometries are sensitive to isotopic labeling. Ultrathin synthetic pore free LB membranes exhibit strong selectivity for isotopically labeled polymers and size discrimination. Expanding these results to understand as well as construct new ultrathin membranes for ion, isotope, and gas separation[16−19,23] and biologically relevant systems for fundamental studies provides areas of active interest.

Supporting Information Available: A detailed experimental description. This material is available free of charge via the Internet at http://pubs.acs.org.

LA001580G

(42) Nishi, T. J. *Macromol. Sci. Phys.* **1980**, *B17*, 517.

(43) Hammouda, B.; Briber, R. M.; Bauer, B. J. *Polymer* **1992**, *33*, 1785.

(44) Han, C. C.; Bauer, B. J.; Clark, J. C.; Muroga, Y.; Matsushita, Y.; Okada, M.; Qui, T. C.; Chang, T. H.; Sanchez, I. C. *Polymer* **1988**, *29*, 2002.